

24. C. A. Wilson, R. K. Grubbs, S. M. George, *Chem. Mater.* **17**, 5625 (2005).
25. A. Fernández, L. R. Scott, *Phys. Rev. Lett.* **91**, 018102 (2003).
26. F. Cordier, S. Grzesiek, *J. Mol. Biol.* **317**, 739 (2002).
27. F. R. N. Gurd, P. E. Wilcox, *Adv. Protein Chem.* **11**, 311 (1956).
28. F. H. Arnold, B. L. Haymore, *Science* **252**, 1796 (1991).
29. J. T. Kellis, R. J. Todd, F. H. Arnold, *Nat. Biotechnol.* **9**, 994 (1991).
30. K. H. Gustavson, *Nature* **182**, 1125 (1958).
31. K. S. J. Rao, G. V. Rao, *Mol. Cell. Biochem.* **137**, 61 (1994).
32. H. Sun, H. Li, R. A. Weir, P. J. Sadler, *Angew. Chem. Int. Ed.* **37**, 1577 (1998).
33. T. Handel, W. F. DeGrado, *J. Am. Chem. Soc.* **112**, 6710 (1990).
34. Generally, in our ALD process, ZnO deposition has shown relatively poor self-limiting features. At longer exposure times, the process shows parasitic chemical vapor deposition (high film thickness with relatively poor uniformity). Therefore, in case of ZnO, an exposure of only 5 s was applied.
35. It has been observed that in the case of the metal-infiltrated silks, the contraction ratio produced by humidity up to 100% or temperature up to 70°C is in an almost negligible range (<3%).
36. A. H. Simmons, C. A. Michal, L. W. Jelinski, *Science* **271**, 84 (1996).
37. Y. Termonia, *Macromolecules* **27**, 7378 (1994).
38. N. Du *et al.*, *Biophys. J.* **91**, 4528 (2006).
39. T. Lefèvre, M.-E. Rousseau, M. Pézolet, *Biophys. J.* **92**, 2885 (2007).
40. Y. Liu, Z. Shao, F. Vollrath, *Nat. Mater.* **4**, 901 (2005).
41. A. L. Let, D. E. Mainwaring, C. Rix, P. Murugaraj, *J. Non-Cryst. Solids* **354**, 1801 (2008).
42. Z. Shao, R. J. Young, F. Vollrath, *Int. J. Biol. Macromol.* **24**, 295 (1999).
43. R. E. Fornes, R. W. Work, N. Morosoff, *J. Polym. Sci. Polym. Phys. Ed.* **21**, 1163 (1983).
44. G. V. Guinea, M. Elices, J. Pérez-Rigueiro, G. R. Plaza, *J. Exp. Biol.* **208**, 25 (2005).
45. D. Porter, F. Vollrath, *Adv. Mater.* **21**, 487 (2009).
46. We thank W. Lee from the Korea Research Institute of Standards and Science in Daejeon, Korea; H. Han from the Department of Material Science and Engineering, Pohang University of Science and Technology in Pohang, Korea; and G.-M. Kim from the Department of Physics, Martin-Luther-University Halle-Wittenberg in Merseburg, Germany, for their helpful discussions on physical and chemical interpretations of mechanical properties, WAXS, NMR spectra, Raman spectra, energy-filtered TEM (EFTEM), and time-of-flight secondary ion mass spectroscopy (TOF-SIMS) data. We also thank J. Woltersdorf, M. Becker, and J. Liu from the Max Planck Institute of Microstructure Physics in Halle, Germany, for EFTEM and Raman measurements. We appreciate TOF-SIMS measurement by M. Krause and help and support in arranging the mechanical properties measurements and TOF-SIMS measurement by M. Petzold from the Fraunhofer Institute for Mechanics of Materials in Halle, Germany. This work has received financial support from the Bundesministerium für Bildung und Forschung (grant FKZ 03X5507) and Deutsche Forschungsgemeinschaft (grants BR 3370/3-1 and Mi 390/17-1).

Supporting Online Material

www.sciencemag.org/cgi/content/full/324/5926/488/DC1
Materials and Methods
SOM Text
Figs. S1 to S11
Tables S1 to S4
References

6 November 2008; accepted 11 March 2009
10.1126/science.1168162

Asymmetric Autocatalysis Triggered by Carbon Isotope ($^{13}\text{C}/^{12}\text{C}$) Chirality

Tsuneomi Kawasaki, Yukari Matsumura, Takashi Tsutsumi, Kenta Suzuki, Masateru Ito, Kenso Soai*

Many apparently achiral organic molecules on Earth may be chiral because of random substitution of the 1.11% naturally abundant ^{13}C for ^{12}C in an enantiotopic moiety within the structure. However, chirality from this source is experimentally difficult to discern because of the very small difference between ^{13}C and ^{12}C . We have demonstrated that this small difference can be amplified to an easily seen experimental outcome using asymmetric autocatalysis. In the reaction between pyrimidine-5-carbaldehyde and diisopropylzinc, addition of chiral molecules in large enantiomeric excess that are, however, chiral only by virtue of isotope substitution causes a slight enantiomeric excess in the zinc alkoxide of the produced pyrimidyl alkanol. Asymmetric autocatalysis then leads to pyrimidyl alcohol with a large enantiomeric excess. The sense of enantiomeric excess of the product alcohol varies consistently with the sense of the excess enantiomer of the carbon isotopically chiral compound.

The limits of knowledge in recognizing and understanding chirality are continually pushed back by innovative methods (1–4). Although the theory of a tetrahedral asymmetric carbon atom with four differing substituents has been understood since the 19th-century work of van't Hoff and LeBel (5–9), molecules for which this characteristic arises solely from carbon isotopic substitution are rare (10). It is not known whether a reactive difference between enantiomers can arise solely from a difference in carbon isotopic substitution. Such an observation has been experimentally inaccessible. Considering that the natural abundance of ^{13}C is ~1.11% on Earth, many organic molecules may be chiral arising from carbon isotope differences in enantiotopic

groups, although the enantiomeric excess arising from this source may be minute (Fig. 1).

There are reports on enantioselective reactions (11, 12) or on a kinetic resolution (13) induced by hydrogen isotope (H/D) replacement, and the use of hydrogen isotopes to explore enzymatic mechanisms is well known (14). In a polymer, isotope chirality (H/D) has been shown to cooperatively control macromolecular helical handedness (15). However, the effect of carbon isotope substitution is expected to be far smaller. Thus, enantioselective reactions induced by molecules that are chiral

solely by virtue of carbon isotope substitution present a challenging problem. To the best of our knowledge, there have been no reports in which carbon isotopically substituted chiral compound induces enantioenrichment in an asymmetric reaction.

Here, we show that asymmetric autocatalysis with amplification of enantioenrichment (16, 17) can be successfully applied to the discrimination between enantiomers that differ solely in substitution of carbon isotopes. Asymmetric autocatalysis has enormous power to recognize molecular chirality (18–22). In the reaction between pyrimidine-5-carbaldehyde **4** and diisopropylzinc (*i*-Pr₂Zn), the zinc alkoxides of the isotopically substituted chiral alcohols **1** to **3** cause a slight enantiomeric excess (ee) in the zinc alkoxide of pyrimidyl alkanol **5**. After autocatalytic amplification of this enantiomeric excess, alkanol **5** accumulates an enhanced ee with a sense that varies consistently with that of the abundant enantiomer of the isotopically substituted chiral compound **1**, **2**, or **3** (Fig. 2).

The isotopically chiral compounds **1** to **3** were synthesized as shown in Fig. 3 (23). First, methyl- ^{13}C -methylphenyl methanol **1** was prepared. To restrict chiral effects to the influence of the carbon isotopic chirality, both enantiomers of **1** were prepared from the same chiral ligand (–)-**8** as shown in Fig. 3, route I. The enantiomers could be synthesized by direct asymmetric dimethylzinc addition to acetophenone using sulfonamide (–)-**8** (24) as a chiral ligand. (*R*)-Alcohol **1** was synthesized using ^{13}C -labeled acetophenone **6** as the substrate. On the other hand, (*S*)-**1** was

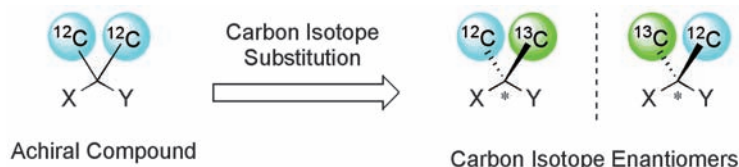


Fig. 1. Generation of chirality by carbon isotope substitution.

Department of Applied Chemistry, Tokyo University of Science, Kagurazaka, Shinjuku-ku, Tokyo 162-8601, Japan.

*To whom correspondence should be addressed. E-mail: soai@rs.kagu.tus.ac.jp

prepared from the ^{13}C -labeled dimethylzinc and unlabeled acetophenone **7** using the same chiral ligand (–)**8**. In route II, asymmetric centers of *tert*-alcohol **1** were introduced by asymmetric epoxidation (25) to the ^{13}C -labeled allyl alcohol **9**, followed by reduction of the tosylate and the epoxide, which afforded the enantiomers of the desired tertiary alcohol **1**.

Next, (*S*)- and (*R*)-1-methyl- ^{13}C -oxy-3-methoxy-2-propanol **2** were synthesized from (*R*)- and (*S*)-glycidyl methyl ether **11** using ^{13}C -labeled sodium methoxide. The stereoinversion reaction (26) of (*S*)-**2** and alcoholysis also afforded the opposite (*R*)-**2**. Thus, both enantiomers **2** could be prepared from (*R*)-**11** as the chiral substrate.

Finally, phenyl-1,2,3,4,5,6- $^{13}\text{C}_6$ -phenylmethanol **3** was synthesized by a diphenyl(1-methylpyrrolidin-2-yl)methanol (DPMPM)-catalyzed asymmetric aryl transfer reaction (27, 28) to the ^{13}C -substituted benzaldehyde **12** to afford **13** with a chiral stereogenic center. Reductive removal of the bromide substituent gave the isotopically substituted enantiomers of diphenylmethanol **3**. The reduction of the aryl bromide via the corresponding highly polar boronic acid facilitated separation of unreacted compounds in each step. The enantiomeric excess of the synthesized alcohols **1** and **2** could be determined from proton nuclear magnetic resonance (^1H -NMR) spectra of their diastereomeric esters of α -methoxy- α -

trifluoromethylphenylacetic acid (MTPA). Because the chemical shift differences for the pair of normal and ^{13}C -labeled groups can be observed, the integration of these peaks shows the diastereomeric excess of these MTPA esters, that is, the enantiomeric excess of the synthesized carbon isotopic chiral alcohols.

We found that the isotopic chirality in alcohols **1** to **3** was successfully discriminated by asymmetric autocatalysis. The results of asymmetric autocatalysis triggered by the carbon isotopically chiral alcohols are shown in Table 1. First of all, we investigated methyl- ^{13}C -methylphenyl methanol **1**, which is a chiral tertiary alcohol formed by the substitution of the ^{13}C -methyl group. In series A1, asymmetric autocatalysis was performed in the presence of (*R*)-**1** with 89% ee; the synthesis of the isotopically substituted alcohol proceeded via route I, including an asymmetric dimethylzinc addition using the same chiral ligand (–)**8**, and production of (*S*)-**5** with 92% ee was observed (entry 1). In turn, when (*S*)-**1** was used as the chiral trigger, (*R*)-**5** with 96% ee was obtained in 95% yield (entry 2). These relationships of absolute configurations between **1** and the resulting **5** are highly reproducible (entries 3 to 8). Additional eight experiments of autocatalytic reaction performed using (*R*)-**1** (table S1, entries 1 to 4) and (*S*)-**1** (entries 5 to 8), have also strongly supported the stereochemical correlations between (*R*)- and (*S*)-alcohol **1** and pyrimidyl alkanol (*S*)- and (*R*)-**5** (23). These results using carbon isotopic chiral *tert*-alcohol **1**, whose enantiomers were synthesized from the same chiral source, clearly indicate that the direction of asymmetric induction is strongly correlated to the carbon isotopic chirality in compound **1**.

Using the single enantiomer (–)**8** in synthesizing both (*R*)- and (*S*)-alcohols **1** excluded the possibility that residual contamination from **8** could have induced the enantiomeric excess of the product alkanol **5**. If trace amounts of **8** in the added sample of alcohol **1** were responsible for the asymmetric induction, we would expect compound **5** to exhibit the same absolute configura-

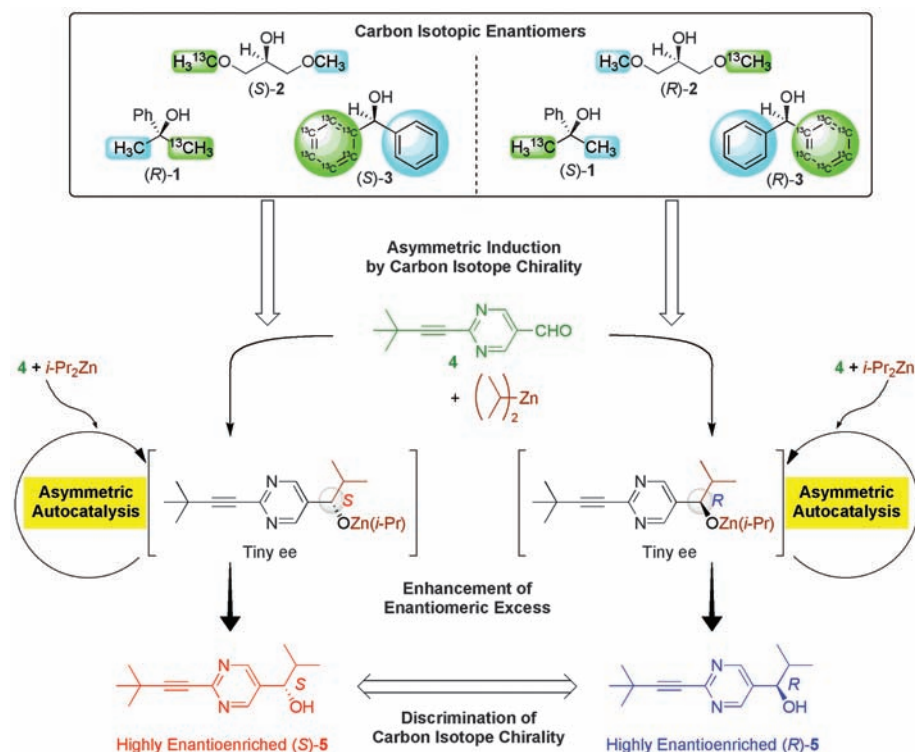
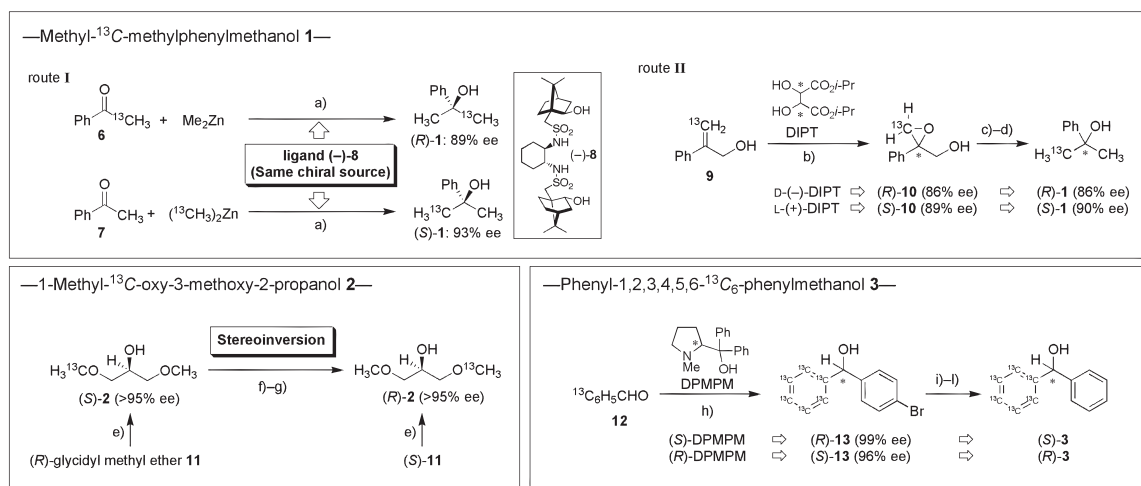


Fig. 2. Discrimination of carbon isotopic chirality by asymmetric autocatalysis.

Fig. 3. Synthetic routes to carbon isotope-modified chiral compounds. a) $\text{Ti}(\text{O}i\text{-Pr})_4$, ligand (–)**8**, toluene or ether; b) diisopropyl tartrate (DIPT), $\text{Ti}(\text{O}i\text{-Pr})_4$, $t\text{-BuOOH}$, CH_2Cl_2 ; c) *p*-toluenesulfonic anhydride, 4-(dimethylamino)pyridine, pyridine; d) LiAlH_4 , ether; e) Na , $^{13}\text{CH}_3\text{OH}$; f) Ph_3P , diisopropyl azodicarboxylate, (*p*- NO_2) $\text{C}_6\text{H}_4\text{CO}_2\text{H}$, tetrahydrofuran (THF); g) K_2CO_3 , MeOH ; h) diphenyl(1-methylpyrrolidin-2-yl)methanol (DPMPM), (*p*- Br) $\text{C}_6\text{H}_4\text{B}(\text{OH})_2$, diethylzinc, toluene then recrystallization; i) chlorotrimethylsilane, Et_3N , THF; j) *n*- BuLi , $\text{B}(\text{OEt})_3$, THF; k) diethylzinc, toluene then H_2O ; l) tetra-*n*-butylammonium fluoride, THF.



tion regardless of the choice of (*R*)- or (*S*)-**1** as a potential trigger. Instead, as confirmed in Table 1, entries 1 to 8, and table S1, entries 1 to 8, (*R*)- and (*S*)-alkanols **5** were obtained reproducibly from adding isotopically chiral (*S*)- and (*R*)-alcohols **1**, respectively, ruling out any role of trace **8**.

In series A2 of Table 1, the enantiomers of *tert*-alcohols **1** were synthesized via route II. In this series, the induction sense was the same as observed in series A1, with high reproducibility-

ty: Chiral alcohol (*R*)-**1** acts as an initiator of (*S*)-alkanol **5** formation (entries 9, 11, 13, and 15), and (*S*)-**1** leads to (*R*)-**5** (entries 10, 12, 14, and 16, respectively). When other samples of (*R*)- and (*S*)-*tert*-alcohol **1**, which were prepared in different vessels, were used as chiral inducers, the same stereochemical outcomes were obtained. To establish reproducibility, we carried out an additional 16 asymmetric autocatalysis experiments, using isotopically chiral (*R*)- and

(*S*)-**1** each 8 times (table S1, entries 9 to 16 and 17 to 24). The results show consistent stereochemical correlations without any exception (23).

To check for chiral influences other than that arising from the isotopically chiral compound, we conducted the autocatalytic reaction induced by the achiral alcohol **1**, which was synthesized by route II using unlabeled **9**. Previously, we have reported spontaneous absolute asymmetric synthesis in the autocatalytic pyrimidine-5-carbaldehyde/diisopropylzinc system (29, 30). That is, under achiral conditions, enantioenriched (*S*)- or (*R*)-alkanol **5** could be obtained by the reaction of aldehyde **4** and *i*-Pr₂Zn in combination with asymmetric autocatalysis. The stochastic behavior of the formation of (*S*)- and (*R*)-alkanol **5** was observed during 84 trials (30). Thus, we considered that if there is no chiral factor, which can induce the chirality in asymmetric autocatalysis, the formation of both (*S*)- and (*R*)-alkanol should be observed. On the other hand, if there were some chiral factors in the reaction, predominant formation of (*S*)- or (*R*)-pyrimidyl alkanol **5** correlated to the chiral factor should be observed. When the autocatalysis was performed in the presence of unlabeled achiral compound **1** prepared using D-(–)-diisopropyl tartrate (DIPT) in the epoxidation step, enantioenriched (*S*)- and (*R*)-alkanol **5** were obtained in three and five instances from eight attempts, respectively. In addition, achiral compound **1**, prepared by using tartrate with the opposite absolute configuration as a chiral ligand, initiated the formation of enantiomers of **5** with equal frequency, that is, four occurrences of *S* and four of *R*. Detailed experimental results of asymmetric autocatalysis in the presence of nonlabeled achiral alcohol **1** are given in table S2 and supporting text (23). Considering the 24 reproducible asymmetric induction results obtained using isotopically chiral **1** (Table 1, entries 9 to 16, and table S1, entries 9 to 24), these observations of both enantiomers of **5** during 16 trials with achiral **1** confirm the absence of any chiral contaminants in the synthesized sample of **1** that can influence the asymmetric autocatalysis.

In series B of Table 1, *sec*-alcohol **2** was used to trigger asymmetric autocatalysis. In the presence of (*S*)-alcohol **2**, enantioselective *i*-Pr₂Zn addition to pyrimidine-5-carbaldehyde **4** led to (*S*)-pyrimidyl alkanol **5** with 97% ee (entry 17). On the other hand, the opposite enantiomer (*R*)-**2** induced the production of (*R*)-**5** with 93% ee (entry 18). When we repeated the experiments, (*S*)- and (*R*)-*sec*-alcohol **2** induced the formation of (*S*)- and (*R*)-alkanol **5** with the same sense of stereochemistry, respectively (entries 19 to 21). To exclude any chiral influence other than that of carbon isotopic chirality, the (*R*)-alcohol **2** used as the chiral initiator in entries 22 to 24 was prepared from the opposite enantiomer (*S*)-**2** by the stereoinversion reaction; the same stereochemical correlation as before was observed in formation of enantioenriched (*R*)-**5**. The reproducibility was further established by an additional 14 asymmetric autocatalysis experiments

Table 1. Chiral discrimination of the carbon isotopically chiral alcohols using asymmetric autocatalysis.

Entry	¹³ C/ ¹² C chiral alcohol (ee)	Pyrimidyl alkanol 5		
		Isolated yield	ee	Configuration
Series A1 ^{††}				
1	(<i>R</i>)- 1 (89% ee)	94	92	<i>S</i>
2	(<i>S</i>)- 1 (93% ee)	95	96	<i>R</i>
3	(<i>R</i>)- 1 (89% ee)	80	88	<i>S</i>
4	(<i>S</i>)- 1 (93% ee)	94	96	<i>R</i>
5	(<i>R</i>)- 1 (89% ee)	96	88	<i>S</i>
6	(<i>S</i>)- 1 (93% ee)	97	94	<i>R</i>
7	(<i>R</i>)- 1 (89% ee)	[not determined]	93 [§]	<i>S</i>
8	(<i>S</i>)- 1 (93% ee)	92	93	<i>R</i>
Series A2 ^{†††}				
9	(<i>R</i>)- 1 (86% ee)	94	94	<i>S</i>
10	(<i>S</i>)- 1 (86% ee)	87	95	<i>R</i>
11	(<i>R</i>)- 1 (86% ee)	93	94	<i>S</i>
12	(<i>S</i>)- 1 (90% ee)	98	93	<i>R</i>
13	(<i>R</i>)- 1 (86% ee)	85	92	<i>S</i>
14	(<i>S</i>)- 1 (84% ee)	93	88	<i>R</i>
15	(<i>R</i>)- 1 (86% ee)	88	89	<i>S</i>
16	(<i>S</i>)- 1 (90% ee)	93	90	<i>R</i>
Series B ^{†††}				
17	(<i>S</i>)- 2 (>95% ee)	92	97	<i>S</i>
18	(<i>R</i>)- 2 (>95% ee)	86	93	<i>R</i>
19	(<i>S</i>)- 2 (>95% ee)	89	92	<i>S</i>
20	(<i>R</i>)- 2 (>95% ee)	89	76	<i>R</i>
21	(<i>S</i>)- 2 (>95% ee)	90	83	<i>S</i>
22 [#]	(<i>R</i>)- 2 (>95% ee)	90	95	<i>R</i>
23 [#]	(<i>R</i>)- 2 (>95% ee)	92	89	<i>R</i>
24 [#]	(<i>R</i>)- 2 (>95% ee)	78	89	<i>R</i>
Series C ^{†††}				
25	(<i>S</i>)- 3 (99% ee)	96	95	<i>S</i>
26	(<i>R</i>)- 3 (96% ee)	96	92	<i>R</i>
27	(<i>S</i>)- 3 (99% ee)	73	94	<i>S</i>
28	(<i>R</i>)- 3 (96% ee)	80	92	<i>R</i>
29	(<i>S</i>)- 3 (99% ee)	84	94	<i>S</i>
30	(<i>R</i>)- 3 (96% ee)	87	92	<i>R</i>
31	(<i>S</i>)- 3 (99% ee)	85	70	<i>S</i>
32	(<i>R</i>)- 3 (96% ee)	80	76	<i>R</i>

*Carbon isotopically chiral initiator **1** was synthesized via route I in Fig. 3. †The molar ratio of **1**:*i*-Pr₂Zn = 0.05:1.05:2.15. Aldehyde **4** and *i*-Pr₂Zn were added in three separate portions. ††Forty-six additional runs were carried out in this way, further confirming the invariance of the relationship between the handedness of alcohol **1**–**3** and that of product **5**, but with a variation in the absolute value of the product ee. In series A1 (8 further runs) with alcohol **1** of 89% ee (*R*) or 93% ee (*S*), the range of product ee was 79 to 94%; for series A2 (16 further runs) with alcohol **1** varying in ee between 84 and 90%, the range of product ee was between 32 and 95%; for series B (14 further runs) with alcohol **2** (*R*) or (*S*) of >95% ee, the range of product ee was between 63 and 88%, and for series C (8 further runs) with alcohol **3** of 99% ee (*S*) or 96% ee (*R*), the range of ee of the product **5** was between 63 and 88%. See table S1 for the full data. †††The enantioenrichment of product alkanol **5** amplifies according to the addition of aldehyde **4** and *i*-Pr₂Zn: For example, in this entry the step-by-step measured ee values of alkanol **5** during three consecutive reactions were 5% ee (after the initial dropwise addition of **4** and *i*-Pr₂Zn), 32% ee (after the second addition), and then 93% ee (after the third addition). †††Carbon isotopically chiral alcohol **1** was synthesized via route II in Fig. 3. †††The molar ratio of **2**:*i*-Pr₂Zn = 0.04:1.8:3.74. Aldehyde **4** and *i*-Pr₂Zn were added in four separate portions. The ee values of **2** were determined from ¹H-NMR of its MTPA-ester. †††(*R*)-Alcohol **2** used as chiral initiator was synthesized by a stereoinversion reaction from (*S*)-**2**. †††The molar ratio of **3**:*i*-Pr₂Zn = 0.025:0.75:1.525. Aldehyde **4** and *i*-Pr₂Zn were added in four separate portions. The ee of **3** was assigned based on the measured ee of **13**.

using isotopically chiral (*S*)- and (*R*)-**2** eight and six times, respectively (table S1, entries 25 to 32 and 33 to 38). The results show the same stereochemical correlations without any exception (23).

Finally, in series C of Table 1, (*S*)- and (*R*)-phenyl-1,2,3,4,5,6-¹³C₆-phenylmethanol **3** were used as chiral initiators of asymmetric autocatalysis. When (*S*)-**3** was used as the chiral trigger, enantioselective addition of *i*-Pr₂Zn to pyrimidine-5-carbaldehyde **4** afforded (*S*)-pyrimidyl alkanol **5** with 95% ee in 96% yield (entry 25). In contrast, the reaction in the presence of (*R*)-**3** gave (*R*)-alkanol **5** with 92% ee (entry 26). These correlations between the ¹³C isotope chirality and the configuration of the produced alkanol **5** also showed strong reproducibility, with (*S*)- and (*R*)-**3** inducing the production of (*S*)- and (*R*)-**5**, respectively (Table 1, entries 27 to 32, and table S1, entries 39 to 46) (23).

In these enantioselective reactions, the initial formation of the zinc alkoxide of the isotopically chiral alcohol tips the enantiomeric balance of the initial *i*-Pr₂Zn addition to aldehyde **4**; thus, a small enantiomeric excess of the zinc alkoxide of **5** is induced. After this step, the subsequent autocatalytic amplification of the small enantiomeric excess causes the zinc alkoxide of **5** to accumulate at enhanced ee, with an absolute configuration tied to that of the ¹³C-labeled chiral alcohol (**1**, **2**, or **3**) used to trigger the process. Thus, the extremely small chiral effect generated by the substitution of the carbon isotope must be responsible, not for the amplification of the enantiomeric excess in the asymmetric autocatalysis, but for the enantioselection observed, that is, for the enantiomer produced in excess in the formation of the initial zinc alkoxide intermediate and therefore in the final production of **5**.

Only minute energy differences can be associated with the isotopically substituted enantiomer of **1**, **2**, or **3** in causing the tiny enantiomeric excess of the alkoxide that triggers the asymmetric autocatalysis arising from the dialkylzinc addition to **4** (Fig. 2). It has been recognized that such minute energy differences are not interpretable with the tools available to structural theory (15, 31). In the initial reaction stage, the minute energy differences have a tiny effect, which is then cooperatively amplified to the final large enantiomeric excess. It is therefore impossible to disclose a structural reason for the difference in frequency of these initial enantiotopic face selectivities. The “cooperation–amplification” effect, which has been discussed regarding the structural effect of hydrogen deuterium chiral substitution in a helical polymer (15), finds reactive analogy in this autocatalytic system. The product handedness is entirely predictable, but the absolute value of the ee varies from run to run. This observation indicates a stochastic influence in the initiation phase biased by the chiral additive. The locally induced enantiomeric excess of zinc alkoxide is then amplified by the normal asymmetric autocatalytic process (32).

The neglected carbon isotopic chirality of many organic compounds on Earth—a characteristic that has largely eluded discrimination using contemporary methods—can thus be discriminated by asymmetric autocatalysis, which is a highly sensitive reaction for recognizing and amplifying the extremely small chiral influence between ¹²C and ¹³C. The method described above may expand the scope of research on carbon isotope chirality in organic molecules in nature (33). Natural enantiomeric excesses in this class of carbon isotopically chiral compounds may be very low, however. The possible role in asymmetric autocatalytic reactions of such compounds with low ee remains to be clarified.

References and Notes

- K. Nakanishi, N. Berova, R. W. Woody, *Circular Dichroism: Principles and Applications* (Wiley, New York, 2000).
- J. Haesler, I. Schindelholz, E. Riguet, C. G. Bochet, W. Hug, *Nature* **446**, 526 (2007).
- L. A. Nafie, T. B. Freedman, *Enantiomer* **3**, 283 (1998).
- L. D. Barron, *Nature* **238**, 17 (1972).
- K. Mislow, *Top. Stereochem.* **22**, 1 (1999).
- M. Tsukamoto, H. B. Kagan, *Adv. Synth. Catal.* **344**, 453 (2002).
- I. Weissbuch, L. Addadi, M. Lahav, L. Leiserowitz, *Science* **253**, 637 (1991).
- A. Eschenmoser, *Science* **284**, 2118 (1999).
- J. R. Cronin, S. Pizzarello, *Science* **275**, 951 (1997).
- M. A. Evans, J. P. Morken, *J. Am. Chem. Soc.* **124**, 9020 (2002).
- H. Pracejus, *Tetrahedron Lett.* **7**, 3809 (1966).
- I. Sato, D. Omiya, T. Saito, K. Soai, *J. Am. Chem. Soc.* **122**, 11739 (2000).
- A. Horeau, A. Nouaille, K. Mislow, *J. Am. Chem. Soc.* **87**, 4957 (1965).
- D. Arigoni, E. L. Eliel, *Top. Stereochem.* **4**, 127 (1969).
- M. M. Green *et al.*, *Angew. Chem. Int. Ed.* **38**, 3139 (1999).
- K. Soai, T. Shibata, H. Morioka, K. Choji, *Nature* **378**, 767 (1995).
- I. Sato, H. Urabe, S. Ishiguro, T. Shibata, K. Soai, *Angew. Chem. Int. Ed.* **42**, 315 (2003).
- T. Shibata *et al.*, *J. Am. Chem. Soc.* **120**, 12157 (1998).
- K. Soai *et al.*, *J. Am. Chem. Soc.* **121**, 11235 (1999).
- T. Kawasaki *et al.*, *J. Am. Chem. Soc.* **128**, 6032 (2006).
- D. G. Blackmond, C. R. McMillan, S. Ramdeehul, A. Schorm, J. M. Brown, *J. Am. Chem. Soc.* **123**, 10103 (2001).
- D. Lavabre, J.-C. Micheau, J. R. Islas, T. Buhse, *Top. Curr. Chem.* **284**, 67 (2008).
- Materials, methods, and additional experimental results of asymmetric autocatalysis are available as supporting material on Science Online.
- O. Prieto, D. J. Ramón, M. Yus, *Tetrahedron Asymmetry* **14**, 1955 (2003).
- T. Katsuki, K. B. Sharpless, *J. Am. Chem. Soc.* **102**, 5974 (1980).
- O. Mitsunobu, M. Yamada, *Bull. Chem. Soc. Jpn.* **40**, 2380 (1967).
- K. Soai, S. Niwa, *Chem. Rev.* **92**, 833 (1992).
- G. Zhao, X. Li, X. Wang, *Tetrahedron Asymmetry* **12**, 399 (2001).
- K. Soai *et al.*, *Tetrahedron Asymmetry* **14**, 185 (2003).
- T. Kawasaki, K. Suzuki, M. Shimizu, K. Ishikawa, K. Soai, *Chirality* **18**, 479 (2006).
- M. M. Green, C. Khatri, N. C. Peterson, *J. Am. Chem. Soc.* **115**, 4941 (1993).
- T. Shibata, S. Yonekubo, K. Soai, *Angew. Chem. Int. Ed.* **38**, 659 (1999).
- B. Barabás, L. Caglioti, K. Micskei, C. Zucchi, G. Pályi, *Orig. Life Evol. Biosph.* **38**, 317 (2008).
- This work was supported by a Grant-in-Aid for Scientific Research from The Ministry of Education, Culture, Sports, Science and Technology (MEXT). The authors are grateful to the reviewers for helpful discussions.

Supporting Online Material

www.sciencemag.org/cgi/content/full/1170322/DC1
Materials and Methods
SOM Text
Figs. S1 to S11
Schemes S1 to S10
Tables S1 and S2

29 December 2008; accepted 3 March 2009
Published online 26 March 2009;
10.1126/science.1170322
Include this information when citing this paper.

A Global View of the Lithosphere-Asthenosphere Boundary

Catherine A. Rychert* and Peter M. Shearer

The lithosphere-asthenosphere boundary divides the rigid lid from the weaker mantle and is fundamental in plate tectonics. However, its depth and defining mechanism are not well known. We analyzed 15 years of global seismic data using *P*-to-*S* (*Ps*) converted phases and imaged an interface that correlates with tectonic environment, varying from 95 ± 4 kilometers beneath Precambrian shields and platforms to 81 ± 2 kilometers beneath tectonically altered regions and 70 ± 4 kilometers at oceanic island stations. High-frequency *Ps* observations require a sharp discontinuity; therefore, this interface likely represents a boundary in composition, melting, or anisotropy, not temperature alone. It likely represents the lithosphere-asthenosphere boundary under oceans and tectonically altered regions, but it may constitute another boundary in cratonic regions where the lithosphere-asthenosphere boundary is thought to be much deeper.

Mapping the depth and character of the lithosphere-asthenosphere boundary with existing seismic methods has proven

to be a challenge. Global surface-wave studies (*I–4*) image rigid lithospheres that increase in thickness from oceans to continents at broad